Electronic Supplementary Material (ESI) for CrystEngComm.
This journal is © The Royal Society of Chemistry 2023

Supporting Information

Selective synthesis of two-dimensional semiconductive coordination polymers with silver–sulfur network

Ryohei Akiyoshi,[a] Akinori Saeki,[b] Kazuyoshi Ogasawara,[a] Hirofumi Yoshikawa,[c] Yuiga Nakamura,[d] and Daisuke Tanaka*[a]

[a] Department of Chemistry, School of Science, Kwansei Gakuin University, 1 Gakuen Uegahara, Sanda, Hyogo 669-1330, Japan

[b] Department of Applied Chemistry, Graduate School of Engineering, Osaka University, 2-1 Yamadaoka, Suita, Osaka 565-0871, Japan

[c] Department of Nanotechnology for Suitable Energy, School of Engineering, Kwansei Gakuin University, 1 Gakuen Uegahara, Sanda, Hyogo 669-1330, Japan

[d] Japan Synchrotron Radiation Research Institute (JASRI), 1-1-1 Kouto, Sayo-cho, Sayo-gun, Hyogo 679-5198, Japan

Email: dtanaka@kwansei.ac.jp

Table of Contents

Experimental Section

Experimental

Materials

CF_3COOAg (≥97.0%), 1,3-thiazolidine-2-thione (Htzdt) (≥95.0%), acetone (≥99.0%), and methanol (≥99.5%) were obtained from Fujifilm Wako Pure Chemical Industries, Osaka, Japan. All chemicals and solvents employed in syntheses were of reagent grade and were used without further purification.

Synthesis

$[Ag(tzdt)]_n$ (KGF-24)

CF_3COOAg (132.5 mg, 0.6 mmol) and Htzdt (71.5 mg, 0.6 mmol) were dissolved in acetone (8.0 mL) and sealed in a 16-mL autoclave. The solution was heated to 80 °C for 48 h. Then, the container was cooled to 30 °C for 12 h. The residue was collected by centrifugation (4800 rpm, 5 min), followed by washing with acetone and methanol in turn. The resulting solid was dried under vacuum to obtain the product as colorless plate crystals (65.6 mg, 48.4%). Anal. $C_3H_4AgNS_2$: calcd. C 15.94, H 1.78, N 6.20; found. C 15.94, H 1.79, 6.02.

$[Ag_2(tzdt)(TFA)]_n$ (KGF-25)

KGF-25 was synthesized from CF_3COOAg (265.1 mg, 1.2 mmol) and Htzdt (71.5 mg, 0.6 mmol) using the same procedure as that used for **KGF-24**. The product was collected as colorless plate crystals (89.6 mg, 33.4%). Anal. $C_5H_4Ag_2F_3NO_2S_2$: calcd. C 13.44, H 0.90, N 3.13; found. C 13.67, H 0.79, N 3.12.

Methods

Elemental analysis

Elemental analysis was performed by A-Rabbit-Science Japan Co., Ltd.

Single crystal X-ray diffraction (SCXRD) measurement

SCXRD data for **KGF-24** were collected on a Hybrid Pixel Array Detector with synchrotron radiation (λ = 0.41420 Å) at the BL02B1 beamline of the SPring-8 synchrotron radiation facility. The SCXRD data for **KGF-25** were collected on a Rigaku Saturn CCD diffractometer with Mo-K*a* radiations (λ = 0.71075 Å). The diffraction profiles were integrated using the CrysAlisPro software. The crystal data were solved by directed methods using the SHELXT program and refined with SHELXL.[1,2] Anisotropic thermal parameters were used to refine all non-H atoms. All calculations were conducted using the Olex2 crystallographic software package.[3]

Powder X-ray diffraction (PXRD) measurement

PXRD patterns were obtained on a Rigaku MiniFlex600 diffractometer at 40 kV and 15 mA using

a Cu-target tube. The samples were examined without grinding, and the data were collected in the 2–50° 2θ range using Cu-Kα radiation (λ = 1.54187 Å).

Thermogravimetric (TG) analysis

TG analyses were performed on a Shimadzu DTG-60 instrument in the temperature range 30–500 °C at 10 °C min^{-1} under N_2 atmosphere.

Diffuse-reflectance ultraviolet–visible–near-infrared (DR–UV–Vis–NIR) spectroscopy

DR–UV–Vis–NIR spectroscopy was performed using a SHIMADZU UV-3600 UV–Vis–NIR spectrophotometer from 200 to 600 nm. $BaSO_4$ powder was used as a non-adsorbing background. The bandgaps were calculated through the Kubelka–Munk (KM) function using the following equation:

$$\frac{K}{S} = F(R) = \frac{(1-R)^2}{2R}$$

where K is the absorption coefficient, S is a scattering factor, R is the reflectance, and $F(R)$ is the KM function. The band gap was determined from the Tauc plot with $[F(R) \times hv]^{1/2}$ vs. hv by extrapolating the linear region to the abscissa.

Time-resolved microwave conductivity (TRMC) measurement

Crystalline samples on adhesive tape on a quartz substrate were set in a resonant cavity and probed using continuous microwave radiation at ~9.1 GHz. The third harmonic generation (THG; 355 nm) of a Nd:YAG laser (Continuum Inc., Surelite II, 5–8 ns pulse duration, 10 Hz) was used as the excitation source (incident photon density I_0 = 9.1 × 10^{15} – 4.6 × 10^{14} photons cm^{-2} $pulse^{-1}$).

Photoelectron yield spectroscopy (PYS)

Crystalline samples on a conductive carbon tape were subjected to PYS using a Bunko Keiki BIP-KV202GD instrument.

First- principles calculation

First-principles calculations were performed using CASTEP 2020 (20.1.0.5). We calculated the band structure and density of state using the generalized gradient approximation functional proposed by Perdew, Burke, and Ernzerhof (PBE) for the exchange correlation potential. Atomic positions were relaxed to enable minimization of the potential energy. The energy tolerance for the electronic structure calculations was 5 × 10^{-7} eV, and that for ionic relaxation was 5 × 10^{-6} eV. The pseudopotential plane-wave method was ultrasoft in PBE, the plane-wave cut-off was set to 570 eV for **KGF-24** and 630 eV for **KGF-25**, and the Brillouin zone was sampled with a 5 × 8 × 6 *k*-point mesh for **KGF-24** and 4 × 5 × 7 *k*-point mesh for **KGF-25**.

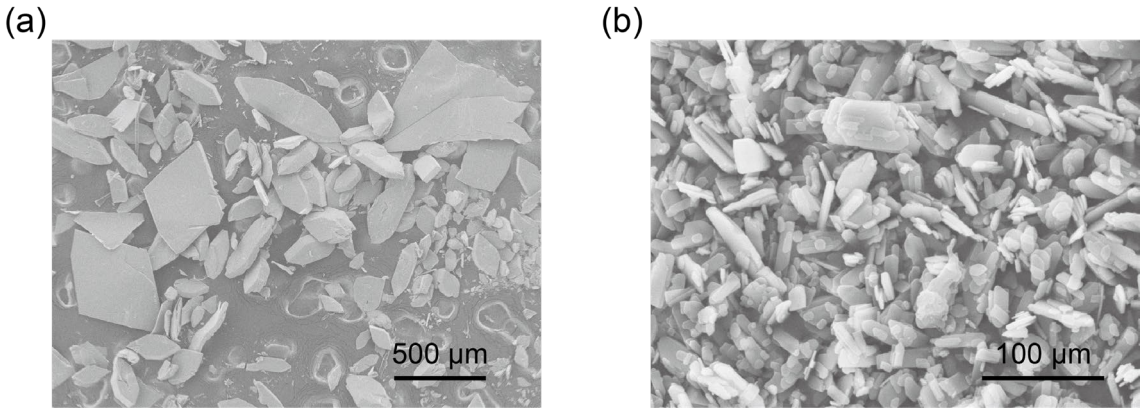

Fig. S1. SEM images showing textures of (a) **KGF-24** and (b) **KGF-25**.

Table S1. Crystallographic data for **KGF-24** and **KGF-25**.

Compound	**KGF-24**	**KGF-25**
Formula	$C_3H_4AgNS_2$	$C_5H_4Ag_2F_3NO_2S_2$
Formula weight	226.06	446.95
T / K	150	150
Crystal system	Monoclinic	Monoclinic
Space group	$P2_1/c$	$P2_1/c$
a / Å	11.1792 (3)	12.4028 (3)
b / Å	6.3833 (1)	10.0914 (3)
c / Å	7.9535 (2)	7.3468 (2)
α / deg	90	90
β / deg	104.230 (3)	91.801 (2)
γ / deg	90	90
V / Å^3	550.15 (2)	919.08 (4)
Z	4	4
ρ_{calc} / g cm^{-3}	2.729	3.230
μ / mm^{-1}	5.084	4.737
F_{000}	432.0	840.0
R_1 ($I > 2\sigma(I)$)	0.0487	0.0357
R_1 (all data)	0.0495	0.0463
wR_2 ($I > 2\sigma(I)$)	0.1439	0.0841
wR_2 (all data)	0.1451	0.0918
GOF	1.101	1.031
CCDC number	2236352	2236353

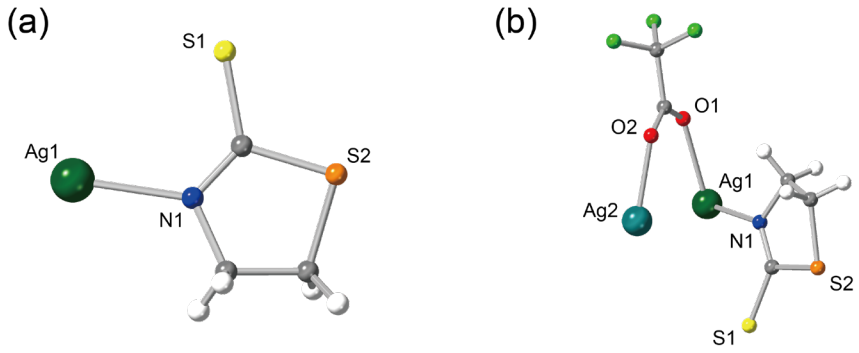

Fig. S2. Asymmetric unit of (a) **KGF-24** and (b) **KGF-25**. Color code: Ag1; dark green, Ag2; light green, S1; yellow, S2; orange, N; blue, C; grey, F; green, H; white.

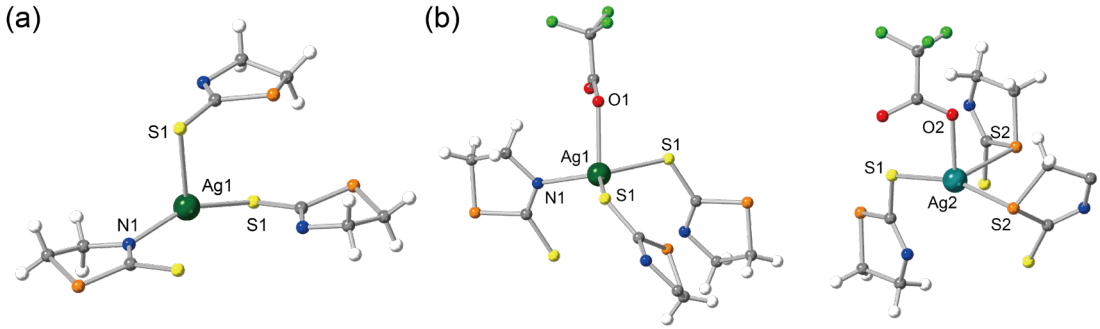

Fig. S3. Structures around Ag(I) center of (a) **KGF-24** and (b) **KGF-25**.

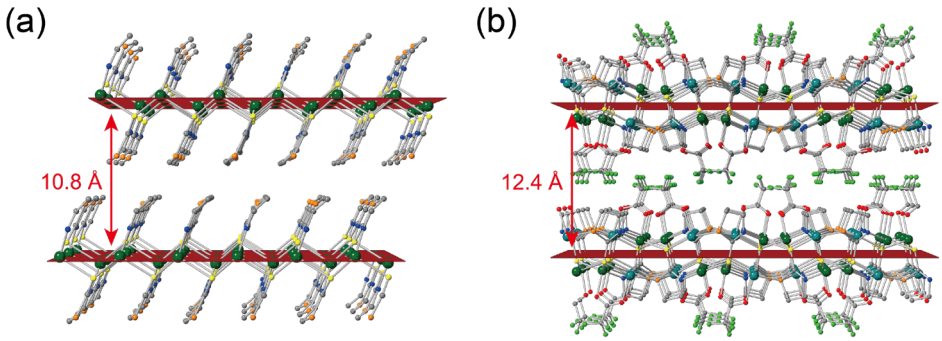

Fig. S4. Packing structures of 2D layers indicating interlayer distance for (a) **KGF-24** and (b) **KGF-25**.

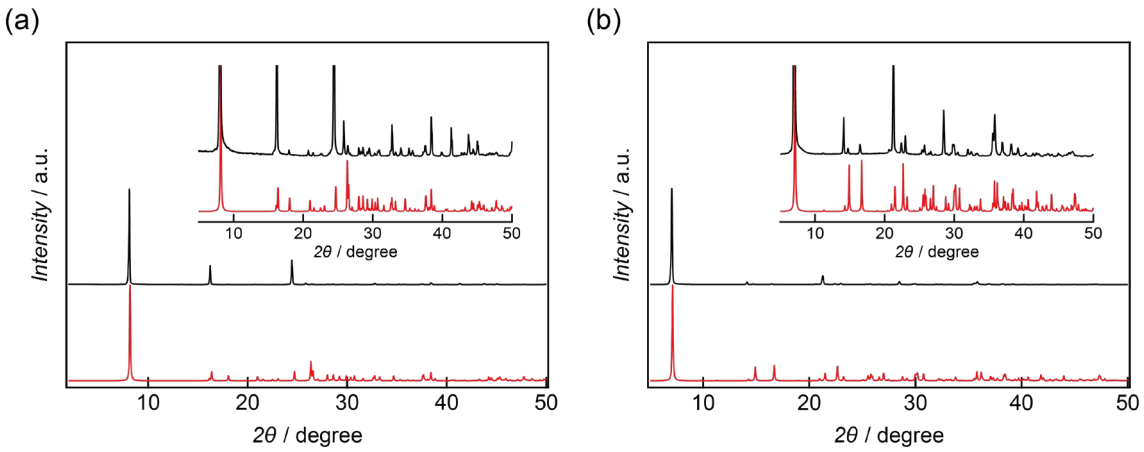

Fig. S5. PXRD pattern of (a) **KGF-24** and (b) **KGF-25**. Inset shows enlarged PXRD pattern (red: simulation pattern obtained from SCXRD, black: experimental pattern).

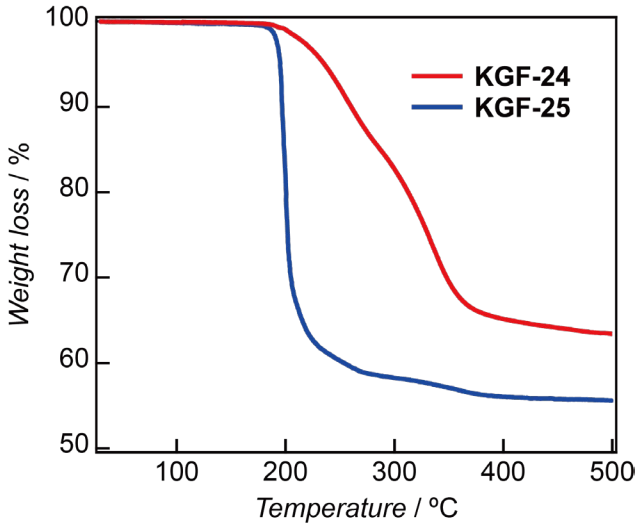

Fig. S6. TG results for **KGF-24** (red) and **KGF-25** (blue) in the temperature range 30–500 °C.

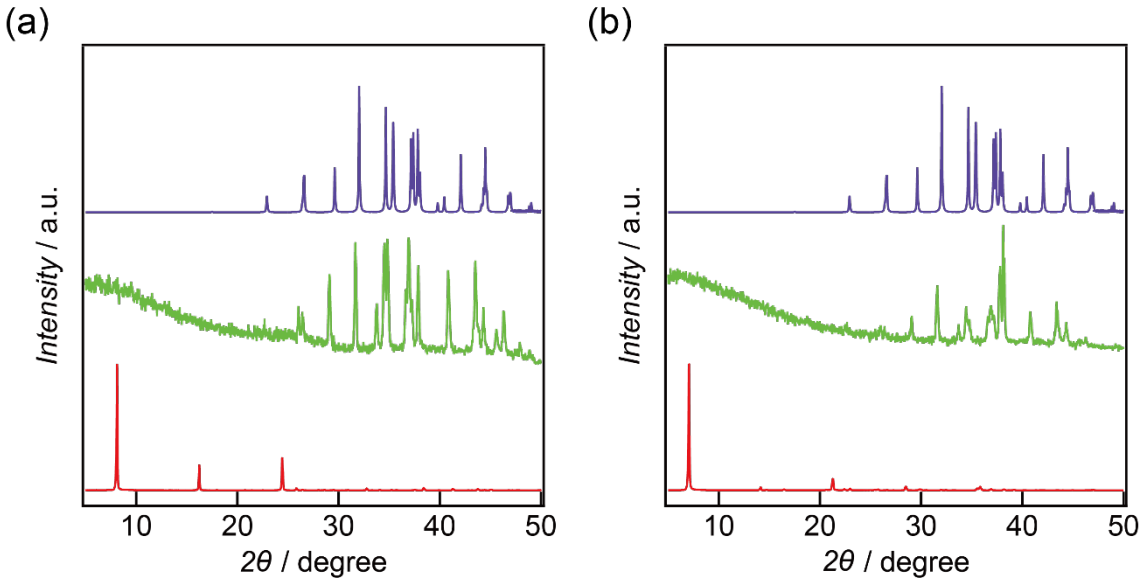

Fig. S7. PXRD pattern of (a) **KGF-24** and (b) **KGF-25** after heating to 500 ℃ (red: as-synthesized, green: products after decomposition, purple: simulation pattern for Ag_2S).

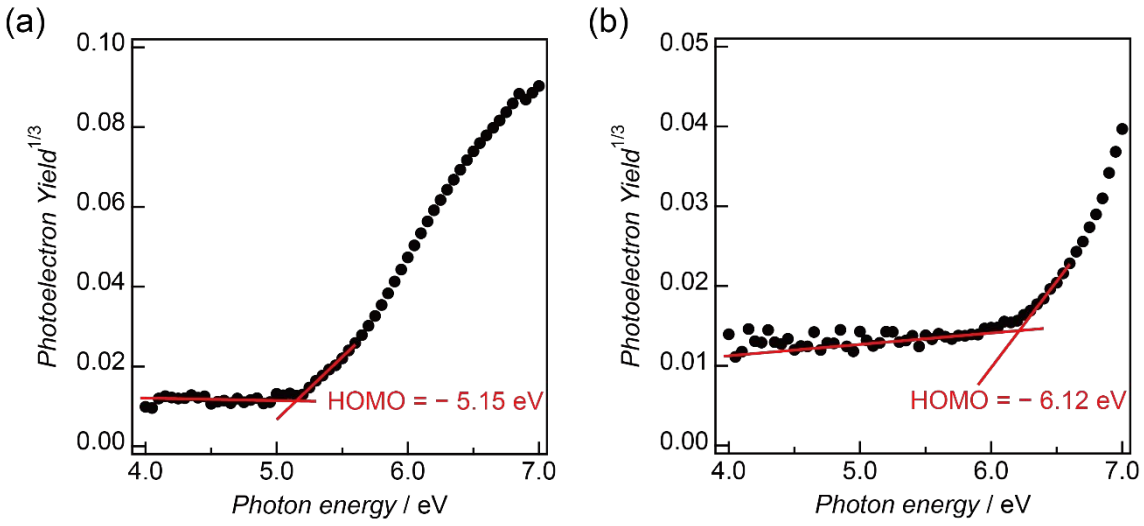

Fig. S8. PYS results of (a) **KGF-24** and (b) **KGF-25**.

Table S2. List of TRMC results for photoconductive CPs and MOFs.

Compound	$\varphi\Sigma\mu_{max}$ / $cm^2\ V^{-1}\ s^{-1}$	Reference
$[Pb_3ttc_2 \cdot 2H_2O]_n$	7.4×10^{-5}	S4
$[Pb(tadt)]_n$	4.9×10^{-5}	S5
$[Sn_2(Httc)_2 \cdot MeOH]_n$	1.8×10^{-5}	S6
$[Ag_2Httc]_n$	1.6×10^{-4}	S7
$[AgH_2ttc]_n$	2.7×10^{-5}	S7
$[Ag_3ttc]_n$	2.8×10^{-5}	S7
$Mn_2(DSBDC)$	2.0×10^{-5}	S8
$Cu_4^{I}Cu_2^{II}Br_4(pyr\text{-}dtc)_4$	9.0×10^{-5}	S9
$Zn_2(TTFTB)$	3.0×10^{-5}	S10
H_4TTFTB	9.0×10^{-6}	S10
$[Ag(tzdt)]_n$ (**KGF-24**)	3.6×10^{-5}	This work
$[Ag(tzdt)(TFA)]_n$ (**KGF-25**)	2.2×10^{-5}	This work

H_3ttc: trithiocyanuric acid: H_2tadt: 1,3,4-thiadiazole-2,5-dithiol: H_4DSBDC: 2,5-disulfhydrylbenzene-1,4-dicarboxylic acid; TTFTB: tetrathiafulvalene-tetrabenzoate.

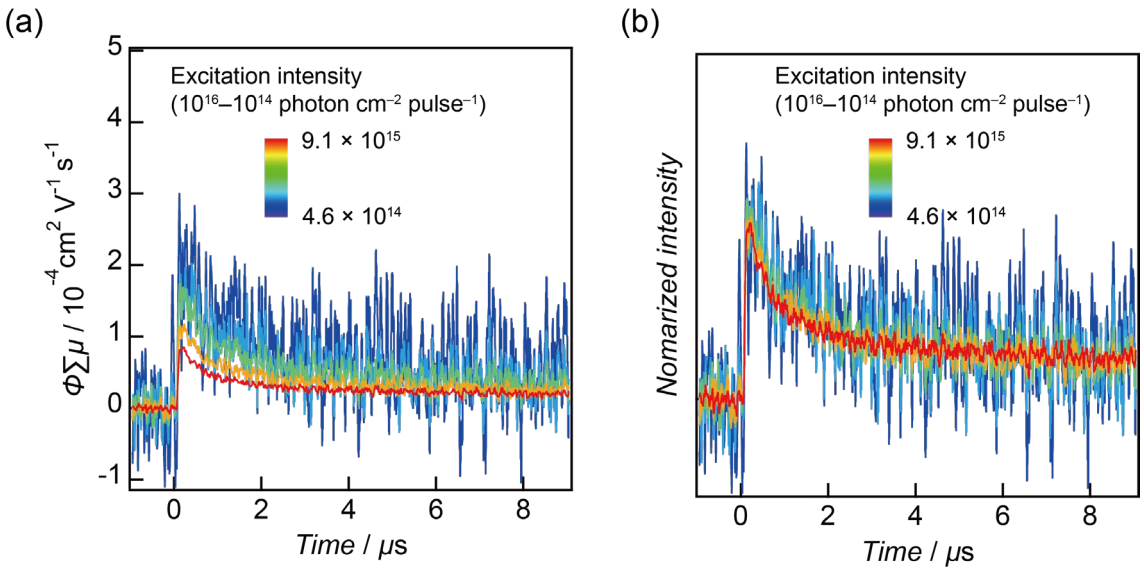

Fig. S9. (a) Excitation intensity dependence of TRMC experiments for **KGF-24**. (b) Normalized results.

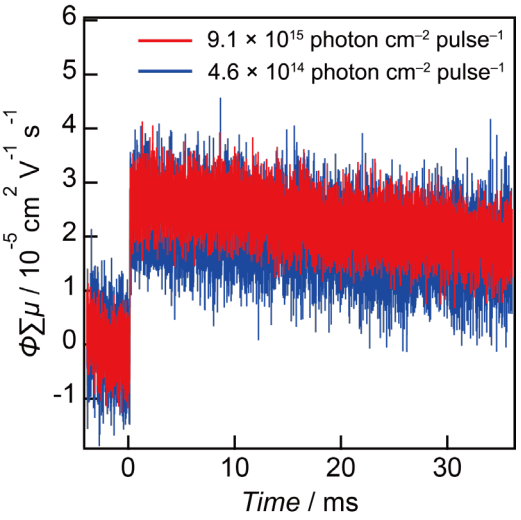

Fig. S10. Excitation intensity dependence of TRMC experiments for **KGF-25**.

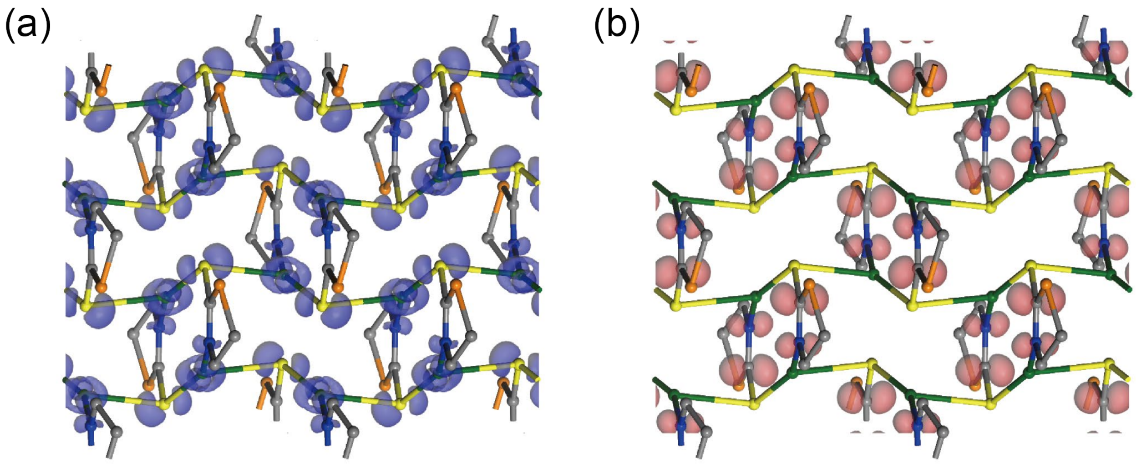

Fig. S11. Distribution of (a) VBM and (b) CBM for **KGF-24**. H atoms are omitted for clarity.

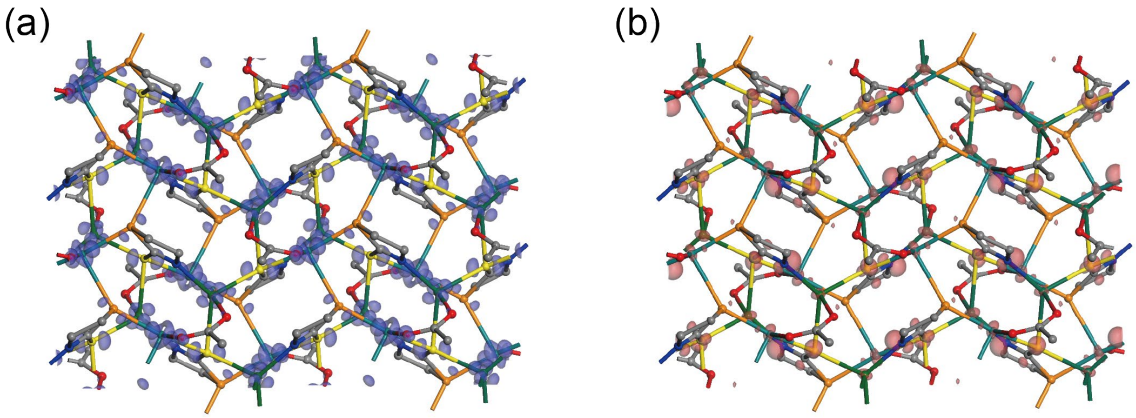

Fig. S12. Distribution of (a) VBM and (b) CBM for **KGF-25**. H and F atoms are omitted for clarity.

References

S1. G. M. Sheldrick, *Acta Cryst.*, 2008, **A64**, 112–122.

S2. G. M. Sheldrick, *Acta Cryst.*, 2015, **C71**, 3–8.

S3. O. V. Dolomanov, L. J. Bourhis, R. J. Gildea, J. A. K. Howard and H. Puschmann, *J. Appl. Cryst.*, 2009, **42**, 339–341.

S4. Y. Kamakura, P. Chinapang, S. Masaoka, A. Saeki, K. Ogasawara, S. R. Nishitani, H. Yoshikawa, T. Katayama, N. Tamai, K. Sugimoto and D. Tanaka, *J. Am. Chem. Soc.*, 2020, **142**, 27–32.

S5. Y. Kamakura, C. Sakura, A. Saeki, S. Masaoka, A. Fukui, D. Kiriya, K. Ogasawara, H. Yoshikawa and D. Tanaka, *Inorg. Chem.*, 2021, **60**, 5436–5441.

S6. Y. Kamakura, S. Fujisawa, K. Takahashi, H. Toshima, Y. Nakatani, H. Yoshikawa, A. Saeki, K. Ogasawara and D. Tanaka, *Inorg. Chem.*, 2021, **60**, 12691–12695.

S7. T. Wakiya, Y. Kamakura, H. Shibahara, K. Ogasawara, A. Saeki, R. Nishikubo, A. Inokuchi, H. Yoshikawa and D. Tanaka, *Angew. Chem. Int. Ed.*, 2022, **61**, e202203151.

S8. T. C. Narayan, T. Miyakai, S. Seki and M. Dinca, *J. Am. Chem. Soc.*, 2012, **134**, 12932–12935.

S9. T. Okubo, H. Anma, N. Tanaka, K. Himoto, S. Seki, A. Saeki, M. Maekawa and T. Kuroda-Sowa, *Chem. Commun.*, 2013, **49**, 4316–4318.

S10. L. Sun, T. Miyakai, S. Seki and M. Dinca, *J. Am. Chem. Soc.*, 2013, **135**, 8185–8188.